Development 129, 2367-2379 (2002)
Printed in Great Britain © The Company of Biologists Limited 2002
DEV4597

Depletion of definitive gut endoderm in *Sox17*-null mutant mice

Masami Kanai-Azuma[1,2], Yoshiakira Kanai[1,*], Jacqueline M. Gad[3], Youichi Tajima[2], Choji Taya[2], Masamichi Kurohmaru[1], Yutaka Sanai[2], Hiromichi Yonekawa[2], Kazumori Yazaki[2], Patrick P. L. Tam[3] and Yoshihiro Hayashi[1]

[1]Department of Veterinary Anatomy, The University of Tokyo, Yayoi 1-1-1, Bunkyo-ku, Tokyo 113-8657, Japan
[2]The Tokyo Metropolitan Institute of Medical Science, 3-18-22 Honkomagome, Bunkyo-ku, Tokyo 113-8613, Japan
[3]Embryology Unit, Children's Medical Research Institute, Locked Bag 23, Wentworthville, NSW 2145, Australia
*Author for correspondence (e-mail: aykanai@mail.ecc.u-tokyo.ac.jp)

Accepted 26 February 2002

SUMMARY

In the mouse, the definitive endoderm is derived from the epiblast during gastrulation, and, at the early organogenesis stage, forms the primitive gut tube, which gives rise to the digestive tract, liver, pancreas and associated visceral organs. The transcription factors, Sox17 (a Sry-related HMG box factor) and its upstream factors, Mixer (homeobox factor) and Casanova (a novel Sox factor), have been shown to function as endoderm determinants in *Xenopus* and zebrafish, respectively. However, whether the mammalian orthologues of these genes are also involved with endoderm formation is not known. We show that *Sox17*$^{-/-}$ mutant embryos are deficient of gut endoderm. The earliest recognisable defect is the reduced occupancy by the definitive endoderm in the posterior and lateral region of the prospective mid- and hindgut of the headfold-stage embryo. The prospective foregut develops properly until the late neural plate stage. Thereafter, elevated levels of apoptosis lead to a reduction in the population of the definitive endoderm in the foregut. In addition, the mid- and hindgut tissues fail to expand. These are accompanied by the replacement of the definitive endoderm in the lateral region of the entire length of the embryonic gut by cells that resemble the visceral endoderm. In the chimeras, although *Sox17*-null ES cells can contribute unrestrictedly to ectodermal and mesodermal tissues, few of them could colonise the foregut endoderm and they are completely excluded from the mid- and hindgut endoderm. Our findings indicate an important role of *Sox17* in endoderm development in the mouse, highlighting the idea that the molecular mechanism for endoderm formation is likely to be conserved among vertebrates.

Key words: Sox17, Definitive endoderm, Visceral endoderm, Mouse

INTRODUCTION

In the mouse, the definitive endoderm is recruited from the epiblast during gastrulation; following ingression through the primitive streak displaces the visceral endoderm to the extra-embryonic yolk sac (Lawson and Pedersen, 1987; Tam and Beddington, 1992). By early organogenesis, the definitive endoderm forms the epithelium of the primitive gut tube from which the digestive tract, liver, pancreas and associated visceral organs develop (Wells and Melton, 1999). In contrast to the wealth of information on the developmental fate and movement of the endodermal progenitors and the morphogenesis of their derivatives, little is known of the genetic determinants that regulate the specification and differentiation of the definitive endoderm. Mutations that cause the loss of function of genes such as *Fgf8* and *Fgfr1* results in defects in the migration and formation of not only the endoderm but also the mesoderm (Deng et al., 1994; Yamaguchi et al., 1994; Sun et al., 1999). *Gata4* which encodes a zinc-finger transcription factor in the visceral endoderm and foregut endoderm is found to be required for gut closure and heart morphogenesis through the activity of other downstream genes (Molkentin et al., 1997; Narita et al., 1997). The loss of *Hnf3β* (*Foxa2* – Mouse Genome Informatics) activity has resulted in the loss of not only the endoderm of the fore- and midgut as well as other embryonic structures such as the notochord (Ang et al., 1993; Sasaki and Hogan, 1993; Dufort et al., 1998). Mutations of the nodal signalling factors such as *Smad2* (*Madh2* – Mouse Genome Informatics) (Tremblay et al., 2000) and *Fast1* (acts upstream of *Hnf3β*) (Hoodless et al., 2001) lead to a deficiency of definitive endoderm. However, like other mutants, the loss of definitive endoderm is accompanied by severe disruption of the differentiation of other embryonic tissues, which hampers the interpretation of the exact functional requirement for the endodermal lineages.

The *Sry*-related HMG box gene, *Sox17*, belongs to the *Sox*-subgroup F with *Sox7* (Taniguchi et al., 1999) and *Sox18* (Dunn et al., 1995). Sox17 was originally identified as a stage-specific transcription activator during mouse spermatogenesis (Kanai et al., 1996). A detailed analysis of the expression of this gene during embryogenesis reveals an earlier phase of activity in the visceral and definitive endoderm of the post-implantation embryo (this study). To date, about 30 Sox genes are identified in various vertebrate species (Pevny and Lovell-Badge, 1997;

Wegner, 1999; Bowles et al., 2000). Members of this gene family encode transcription factors that regulate the specification of cell types and tissue differentiation, such as the differentiation of the Sertoli cells and the formation of the testis [*Sry* (Koopman et al., 1991); *Sox9* (Foster et al., 1994; Wagner et al., 1994; Bishop et al., 2000; Vidal et al., 2001)], lens formation [*Sox1* (Kamachi et al., 1998; Nishiguchi et al., 1998)], pro-B-lymphocyte proliferation [*Sox4* (Schilham et al., 1996)], the differentiation of the neural crest cells that are progenitors of the enteric neurones [*Sox10* (Pingault et al., 1998; Southard-Smith et al., 1998)] and the differentiation of the chondrocytes that form the cartilage [*Sox5* and *Sox6* (Smits et al., 2001), *Sox9* (Foster et al., 1994; Wagner et al., 1994; Bi et al., 1999)].

Consistent with the general role of Sox genes in lineage differentiation, *Sox17* orthologues in *Xenopus* (*Xsox17α*, *Xsox17β*) (Hudson et al., 1997; Clements and Woodland, 2000) and zebrafish (*Zsox17*) (Alexander and Stainier, 1999) are expressed specifically in the endoderm during gastrulation and play a key role in endoderm formation. The expression of a dominant negative *Xsox17* construct, containing the repressor domain of *Drosophila engrailed*, suppresses endoderm differentiation of vegetal blastomeres, while over-expressing *Xsox17*, in conjunction with the upstream homeobox *mixer* gene, activates the expression of endoderm-specific genes in animal cap tissues (Hudson et al., 1997; Henry and Melton, 1998). In the zebrafish, *casanova*, a novel member of Sox subgroup F that acts upstream of *Zsox17* and mediated by nodal signalling activity, can induce endodermal fate in a cell-autonomous manner, thus indicating a similar role for the *Sox17* orthologue (Dickmeis et al., 2001; Kikuchi et al., 2001; Sakaguchi et al., 2001; Aoki et al., 2002).

To elucidate the function of the mouse *Sox17* gene, the phenotype of the *Sox17*-null mutant embryo was examined during post-implantation development. Mutant embryos are found to be deficient of the definitive endoderm lining the embryonic gut. *Sox17*-null ES cells are unable to compete with the wild-type cells in colonising the gut endoderm of the chimeras. *Sox17* therefore plays a crucial role in the differentiation of the definitive endoderm in the mouse, which is consistent with the concept of evolutionary conservation of *Sox17* function in endodermal development in vertebrates.

MATERIALS AND METHODS

Sox17 targeting and generation of mutant mice

We used the mouse *Sox17* genomic DNA clones which were previously isolated from a 129/SvJ genomic library (Kanai et al., 1996). The 1.4 kb *Eco*RI fragment corresponding to the fourth exon, including C-terminal 53 amino acids and 3′-UTR region of *Sox17*, was inserted into the *Eco*RI site between neo and TK cassettes in pKSloxPNT targeting vector. A 5.4 kb *Eco*RI-*Cla*I fragment, which includes the first exon of the *Sox17* 5′-UTR region was inserted downstream of a neo cassette. The targeting vector linearised by *Sal*I was electroporated into a 129/Sv W9.5 ES cell line as described previously (Tajima et al., 1998). After selection with 350 μg/ml G-418 in ES cell media, 12 $Sox17^{+/-}$ ES clones were recovered from 182 G418-resistant colonies analysed, and germline chimeras were generated from two correctly targeted ES lines (line numbers 2-7, 32-4). As mutant embryos of both lines exhibited the same phenotype, the findings of the 2-7 line and 32-4 line are pooled.

Generation of chimaeras and X-gal staining

We isolated the $Sox17^{-/-}$ ES clone from the 2-7 line by selection with 1 mg/ml G-418 in ES cell media (right panel in Fig. 2B), and generated chimaeric embryos by blastocyst injection into ROSA26 ($Sox17^{+/+}$) mice (Jackson Labs). Embryos were fixed with 1% PFA/0.2% glutaraldehyde/0.02% NP40-PBS and subjected to whole-mount X-gal staining. After the whole-mount samples were photographed under the dissecting microscope, transverse frozen sections were prepared for histological analysis.

Genomic Southern blot analysis and PCR assay

Genomic DNA of ES cells and the tail tip of mice was isolated using a Wizard genomic DNA purification kit (Promega, WI). For embryo DNA, part of the yolk sac or allantois was dissected from each embryo, and genomic DNA was prepared using the same kit. To determine the genotype by Southern blot analysis, DNAs were digested with *Bam*HI, electrophoresed and transferred to a nylon membrane. The blots were hybridised with the ^{32}P-labeled probe of the 1.5 kb *Cla*I-*Bam*HI fragment corresponding to the first exon (its position is indicated by a green bold bar in Fig. 2A). To analyse the genotype of the yolk sac or allantois by PCR, the wild-type *Sox17* DNA (235 bp) and the mutated allele DNA (275 bp) were amplified using the following primers: *Sox17* forward, 5′-CTC TGC CCT GCC GGG ATG GCA CGG AAT CC-3′; *Sox17* reverse, 5′-AAT GTC GGG GTA GTT GCA ATA GTA GAC CGC TGA-3′; the target allele forward (pgk promoter reverse), 5′-GCA GGG GCC CTC GAT ATC AAG CTT GGC TG-3′ (their positions are indicated by red arrowheads in Fig. 2A).

Uptake of horseradish peroxidase

Embryos from a heterozygous cross were dissected at 8.0 and 8.5 days post coitum (dpc) and incubated in Dulbecco's modified Eagle medium containing 10% BSA and horseradish peroxidase (HRP; Sigma type IV, 2 mg/ml) for 30 minutes. After separation of the allantois or a part of the visceral endoderm for genome typing, the embryos were fixed and developed by DAB reaction.

Whole-mount and section in situ hybridisation analyses

Whole-mount and section in situ hybridisation were performed essentially as described previously (Gad et al., 1997; Kanai-Azuma et al., 1999). RNA probes for *Sox17* (Kanai et al., 1996), *Sox7* (Taniguchi et al., 1999), *Shh*, *Ihh* (Echelard et al., 1993), *Ptch* (Motoyama et al., 1998), *Gata4* (Molkentin et al., 1997), *Hnf3α* (*Foxa1* – Mouse Genome Informatics) (Sasaki and Hogan, 1993), *Hnf3β* (Ang and Rossant, 1994), *Hex* (Keng et al., 2000), *Hnf4* (Chen et al., 1994), *Afp* (Constam and Robertson, 2000) (Accession Number, AA1172792), *Cer1* (Shawlot et al., 1998), *Cdx2* (Beck et al., 1995) (Accession Number, AI327188) and *Pdx1* (Guz et al., 1995) were used in this study. Embryos were photographed using a dissecting microscope and then 7 μm transverse frozen sections were prepared. To assess the population of definitive endoderm in the embryonic gut, cell counts were performed on histological sections. 8.5 dpc embryos, prepared for whole mount in situ hybridisation for *Hnf3α* mRNA, were cryosectioned serially at 7 μm. Four samples each of normal and mutant embryos were processed. The number of *Hnf3α*-expressing cells per transverse section was scored on 7-10 randomly selected sections of the anterior and posterior gut endoderm. The data for each sample were expressed as mean and standard deviation.

TUNEL staining and immunohistochemistry

Normal and mutant embryos at 7.75-8.5 dpc were fixed in 4% PFA-PBS for 2 hours, and washed in PBS. The PFA-fixed embryos were treated with TdT enzyme reaction, and then detected with anti-FITC-HRP conjugates by using an in situ apoptosis detection kit (Takara Biomedicals, Japan). After the whole-mount samples were photographed using a dissecting microscope, frozen sections were

prepared. TUNEL-positive cells per transverse section were counted on randomly chosen sections to determine the level of cell apoptosis in the anterior or posterior definitive endoderm.

Immunoblot analysis

Embryos were isolated from a cross between heterozygous parents at 7.5 dpc and a portion of the extra-embryonic region was removed for genome typing. Each embryo was then dissolved in sample buffer and each protein sample (one embryo/lane) was used for SDS-PAGE and immunoblotting analysis using anti-*Sox17*-C17 antibody against synthetic peptides corresponding to amino acids 403 to 419 of the SOX17 protein (Kanai et al., 1996).

Histology

Isolated embryos were fixed in 2.5% glutaraldehyde/0.1 M phosphate buffer (PB) for 4 hours at 4°C. After washing in PBS, they were postfixed in 1% OsO_4 in 0.1 M PB for 2 hours at 4°C. The embryos were then dehydrated and embedded in EPON 812. Serial semi-thin sections (1 μm) were cut and stained with 1% Toluidine Blue.

RESULTS

Dynamic pattern of expression of *Sox17* in the endoderm

During post-implantation mouse development, *Sox17* mRNA is detected first in the visceral endoderm nearest to the ectoplacental cone of the pre-streak stage embryo (Fig. 1A,B) and expression progressively spreads to the entire extra-embryonic visceral endoderm by the early-streak stage (Fig. 1C,D). *Sox17* is not detected in the embryonic visceral endoderm. At the mid-streak stage, *Sox17* is also expressed de novo in the endoderm subjacent to the anterior end of the primitive streak (the broken arrow in Fig. 1E), which coincides with the recruitment of the definitive endoderm (Lawson and Pedersen, 1987; Tam and Beddington, 1992). Concomitant with the displacement of definitive endoderm to the anterior region of the gastrula, the *Sox17* expression domain expands to encompass the endoderm underlying the neural plate of the

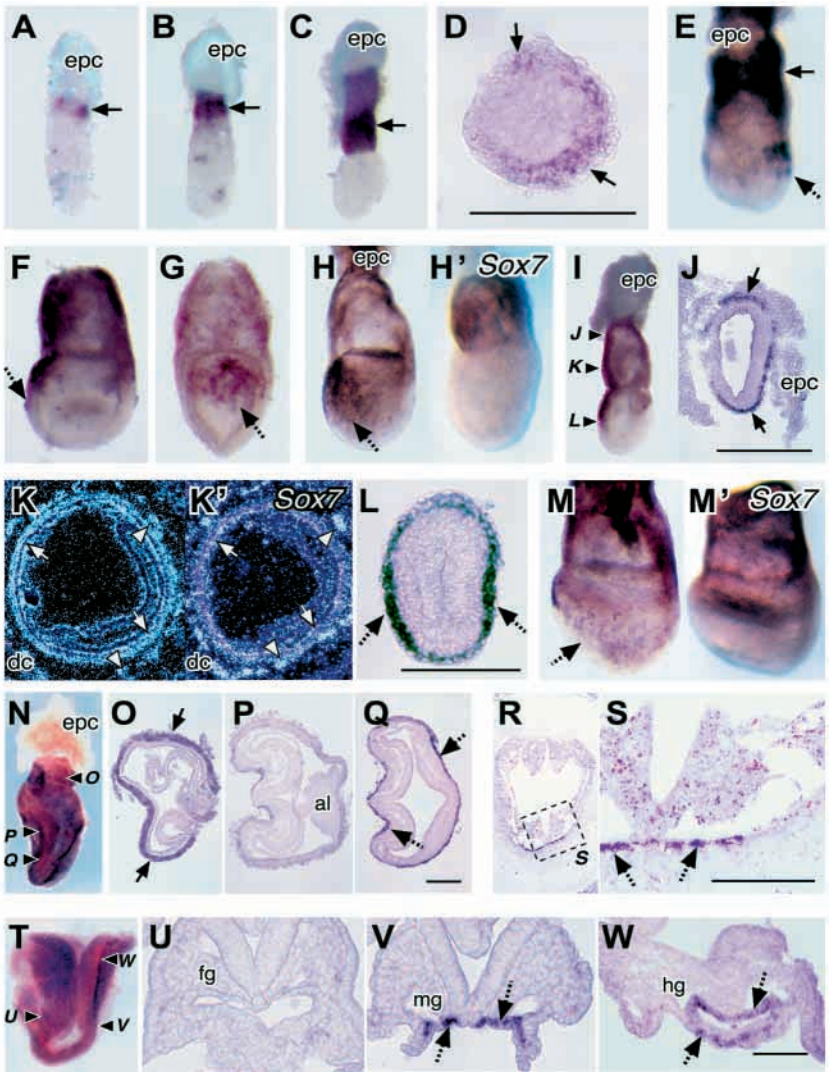

Fig. 1. Expression of *Sox17* and *Sox7* during gastrulation and early organogenesis. (A-C) Pre-streak (A,B; 6 and 6.25 dpc, respectively) and early-streak (C; 6.5 dpc) embryos showing the progressive expansion of *Sox17* expression (arrow) to the whole extra-embryonic region of the visceral endoderm. (D) Transverse section of the extra-embryonic region of an early-streak embryo showing expression of *Sox17* in the visceral endoderm (arrows). (E) Mid-streak (7.0 dpc) stage embryo showing strong expression of *Sox17* in the extra-embryonic visceral endoderm (unbroken arrow) and the endoderm at the anterior end of the primitive streak (broken arrow). (F,G) Lateral (F) and anterior (G) views of early-bud stage (7.5 dpc) embryo revealing *Sox17* expression in the extra-embryonic visceral endoderm and the anterior-most endoderm (broken arrows). (H,H′) Early- to late-bud stage (7.5 dpc) embryos demonstrate the increasing number of *Sox17*-expressing cells in the anterior definitive endoderm (H; broken arrow), but no expression of *Sox7* in the definitive endoderm (H′). (I-L) Embryos at early-bud stage (7.5 dpc): whole embryo (I) and histological section (J) showing strong *Sox17* expression in the visceral endoderm (arrows). Section in situ hybridisation by radioactive riboprobes display strong expression of *Sox17* (K) and *Sox7* (K′) in the parietal (arrowheads) and extra-embryonic visceral endoderm (arrows). Strong *Sox17* expression in the definitive endoderm (L; broken arrows). Planes of sections are indicated by arrowheads in the embryo (I) of a similar developmental stage. (M,M′) Early neural plate stage (7.75 dpc) embryo showing the expansion of *Sox17*-expressing cells (M; broken arrow) and the absence of *Sox7*-expressing cells in the prospective foregut and midgut endoderm (M′). (N-Q) Early headfold stage (8.0 dpc) embryo (arrowheads indicating the plane of the histological sections) showing the descending gradient of *Sox17* expression from the ectoplacental cone (O) to the allantoic region of the visceral endoderm (P), and enhanced expression in the definitive endoderm of the prospective midgut and hindgut (Q). (R,S) Section in situ hybridisation by a DIG-labelled riboprobe showing the regionalised *Sox17* expression (broken arrows) in the posterior definitive endoderm of the 8.25 dpc embryo (four to five somite stage). The broken rectangle in R demarcates the region magnified in S. (T-W) *Sox17* expression in the posterior endoderm of the mid- and hindgut (V,W), but not in the foregut (U) of seven- to eight-somite stage (8.5 dpc) embryo (arrowheads indicating the plane of the histological sections). al, allantois; epc, ectoplacental cone; dc, decidua; fg, foregut; hg, hindgut; mg, midgut. Scale bars: 100 μm.

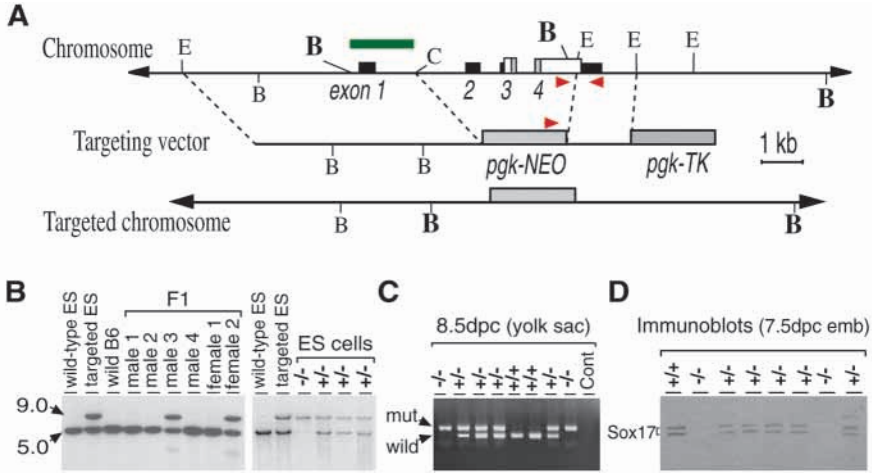

Fig. 2. Targeting a null mutation to the murine *Sox17* gene. (A-C) The *Sox17* targeting strategy. Restriction sites: B, *Bam*HI; E, *Eco*RI; C, *Cla*I. The green bold bar indicates the position of the probe for genomic Southern blot hybridisation using the *Bam*HI-digested samples (mutated allele, 9.0 kb; wild-type allele, 5.0 kb) (genotyping results of ES cells and adult mice are shown in B), while the red arrowheads show the primer positions for genome typing by PCR (results of 8.5 dpc embryos are shown in C). (D) Lack of Sox17 synthesis in mutant 7.5 dpc mouse embryos revealed by immunoblot analysis using anti-Sox17 C17-antibody (Kanai et al., 1996).

early-bud-stage embryo (broken arrows in Fig. 1F-H,I,L). *Sox17* is therefore an early marker that is specifically expressed in the definitive endoderm of the gastrula, in contrast to genes such as *Hex*, *Hnf3β* and *Cer1*, which are expressed simultaneously in the anterior visceral endoderm and the definitive endoderm in the embryonic compartment of the gastrulating mouse embryo. In the neurulating embryo, *Sox17* is expressed in the endoderm of the prospective foregut (Fig.1M). However, by the early headfold stage, expression in the foregut endoderm (Fig. 1P) and in the visceral endoderm near the embryonic region (Fig.1N-P) is reduced. By contrast, endodermal cells in the prospective mid- and hindgut show strong *Sox17* expression (Fig. 1Q). At the three to five somite stage, *Sox17* is expressed in the posterior endoderm (Fig. 1R,S) but by the seven to eight somite stage, *Sox17* is expressed mainly in the endoderm of the midgut and the hindgut invagination of the embryo (Fig. 1T,V,W). *Sox17*-expressing cells are no longer found in the prospective foregut endoderm at these stages (Fig. 1R,U). After 9.0 dpc, *Sox17* expression is also absent from the posterior gut endoderm. The expression of the closely related *Sox7* gene (Taniguchi et al., 1999), overlaps with that of *Sox17* in the extra-embryonic endoderm in the gastrula and neurulation stages (Fig. 1H′,K′,M′). However, *Sox7* is not expressed in the definitive endoderm (Fig. 1H′,M′) or the embryonic gut (data not shown). *Sox17* and *Sox7* function may therefore be redundant in the visceral endoderm, but not in the definitive endoderm.

Gut development is defective in *Sox17*$^{-/-}$ embryos

A null mutation of *Sox17* was generated by replacing exons 2-4 of the gene with a neomycin-resistant cassette, which resulted in the complete loss of SOX17 proteins (Fig. 2A-D). *Sox17*$^{+/-}$ mice were normal and fertile. During embryonic development (until 10.5 dpc), *Sox17*$^{-/-}$ mutant embryos were found in the expected Mendelian ratio: 23.3% (29/124 embryos) at 9.5 dpc and 17.8% (19/107) at 10.5 dpc. No homozygous mutant embryos were found after 10.5 dpc and no live homozygous offspring were recovered among 206 newborn.

Gross anatomical examination of the *Sox17*$^{-/-}$ embryos revealed no discernible defects prior to the early-somite stage (Fig. 3A-C). From 8.5 dpc onwards, *Sox17*$^{-/-}$ embryos can be distinguished by the lack of axis rotation and deteriorating growth (Fig. 3D-F). Development of anterior structures such as neural tube, optic evagination, otic vesicle, branchial arches and heart tube was generally normal until 9.5 dpc (Fig. 3E, and

Fig. 3. Defective gut development of *Sox17*$^{-/-}$ embryos. (A-F) Lateral views of phenotypically normal (+/+,+/–) and mutant (–/–) embryos at 7.5 (late-bud stage; A), 8.0 (headfold stage; B), 8.25 (five- to six-somite stage; C), 8.5 (10- to 12-somite stage; D), 9.5 (E) and 10.5 (F) dpc. The homozygous *Sox17* embryos show no axis turning and poor posterior development from 8.5 dpc onwards. Arrows indicate the plane of histological sections (G-S); unbroken arrow for transverse section and broken arrow for sagittal section. (G) Sagittal and (H,I) parasagittal sections of 8.0 dpc embryos. In the mutant embryo, the visceral endoderm extends further into the prospective gut on the lateral aspects (H,I) than the medial aspects (G) in the posterior region. Arrowheads and arrows mark the frontier of the visceral endodermal cells at the anterior and posterior aspects of the embryo, respectively. (H,I) Insets (right) also show a magnified view of the posterior region. (J,K) Transverse sections at the midgut level of 8.25 dpc embryos. In the mutant (–/–) embryo, the definitive endoderm in the lateral region of the prospective gut is replaced by the cuboidal and vacuolated cells that resemble the visceral endoderm. (L-O) Transverse sections at the fore- and hindgut (L,M) and midgut (N,O) levels of 8.5 dpc embryos. The sections of the heterozygous (+/–) embryo at a similar developmental stage (before axis turning) are shown. In the foregut and hindgut portal of the 8.5 dpc mutant embryos, cells that resemble the visceral endoderm are found in the lateral and ventral regions of the gut tube (L,M). In the lateral region of the open midgut, the endoderm cells are juxtaposed to the mesothelium of the splanchnopleure. By contrast, the mutant (–/–) embryo lacks the layer of splanchnic mesenchyme (red arrows; O) that separates the endoderm from the mesothelium. (P,Q) Sagittal sections of the 9.5 dpc mutant (–/–) embryo, showing normal development of (P) the head, the heart and (Q) the thyroid bud. (R) Transverse sections at the caudal foregut level of 9.5 dpc mutant (–/–) embryos reveals a small foregut, but proper liver bud formation. (S) Transverse sections of the hindgut of 9.5 dpc embryos. In the mutant (–/–) embryo, the hindgut has regressed to a cord-like structure containing significantly fewer endodermal cells. The broken rectangle (J,L,N,P) marks the area shown in the magnified view of the histological section. Arrowheads (J,K,N,O) indicate the border between the definitive endoderm and the presumptive visceral endoderm. ce, coelomic epithelium; da, dorsal aorta; fg, foregut; hg, hindgut; ht, heart; lb, liver bud; mes, mesothelium; sm, splanchnic mesenchyme; thy, thyroid bud. Scale bars: 100 μm.

data not shown). However, growth and morphogenesis of the posterior trunk was severely affected and progressively became disorganised, especially after 9.5 dpc (Fig. 3E,F).

Histological analysis of *Sox17*$^{-/-}$ mutant embryos at 7.0-9.5 dpc revealed that the first morphological defect was found in the definitive endoderm at 8.0 dpc (headfold stage; Fig. 3G-I). No histologically abnormality was detected at the median plane of the mutant embryos (Fig. 3G). However, at the

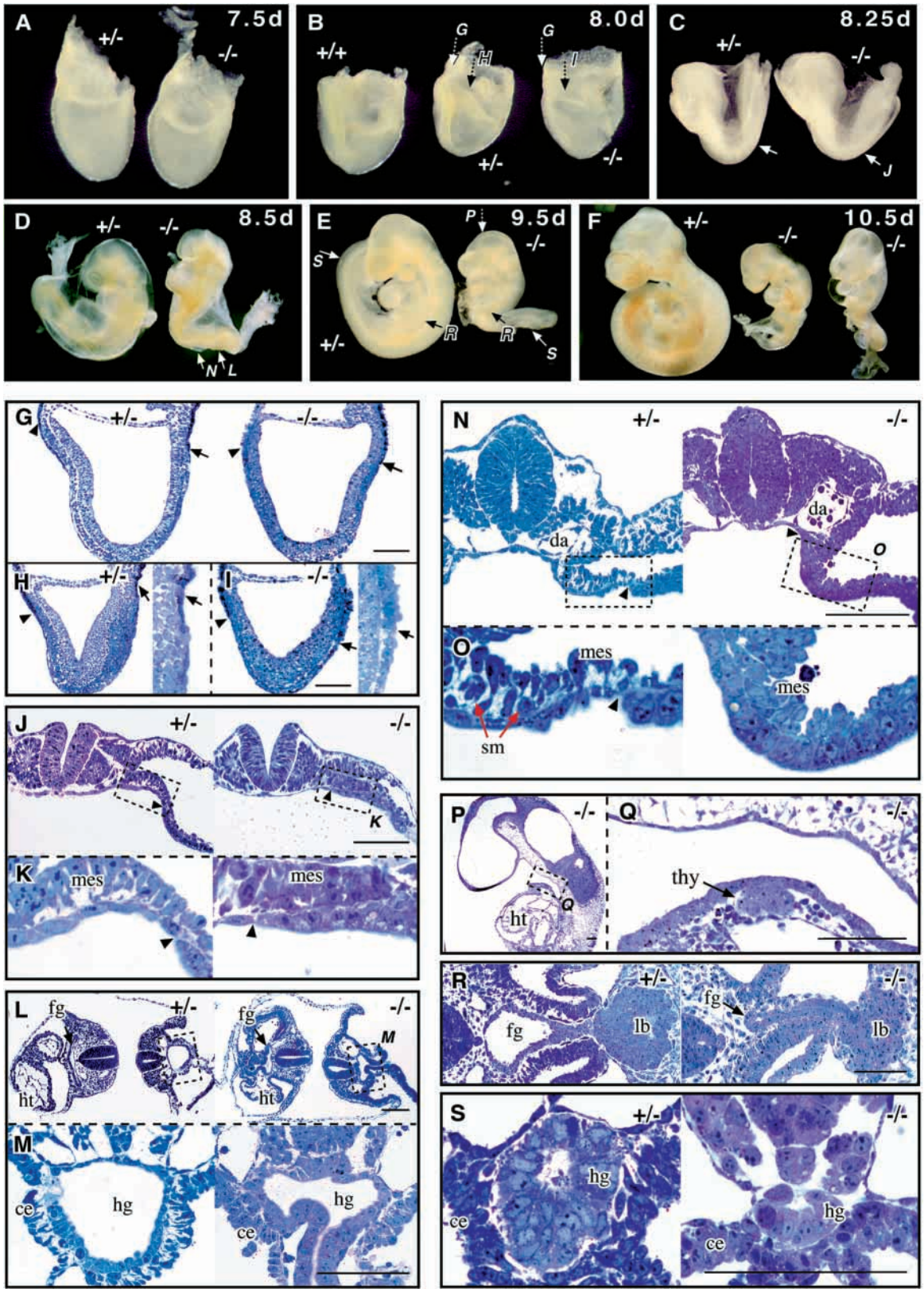

paramedian level, the cuboidal and vacuolated visceral endoderm-like cells were found to extend into the embryonic region in the posterior endoderm, but not in the anterior endoderm, of the mutant embryos (Fig. 3H,I). This suggests a reduced definitive endoderm region at the posterior and lateral regions of the mutant embryos. At 8.25 dpc, the cells in the medial region of the definitive gut endoderm (underneath the notochord and somites) displayed the squamous epithelial morphology typical of the definitive endoderm. However, the cells in the lateral region (beneath the intermediate and lateral plate mesoderm) acquired the cuboidal and vacuolated epithelial appearance reminiscent of that of the visceral endoderm (Fig. 3J,K,N,O). Furthermore, this endodermal layer was juxtaposed directly with the mesothelium of the splanchnopleure and not, as in the wild-type embryo, separated from the mesothelium by a layer of splanchnic mesenchyme (red arrows in Fig. 3O). In the foregut and hindgut portals, visceral endoderm-like cells were found in the lateral and ventral epithelium of the gut (Fig. 3L,M). No obvious histological defects were found in other embryonic structures such as the notochord, somites, neural tube and heart. At 9.5 dpc, *Sox17*$^{-/-}$ mutant embryos display the apparently normal development of the craniofacial structures, the heart (Fig. 3P) and the primordia of the liver and the thyroid gland (Fig. 3Q,R). However, the foregut is reduced in size and deficient of endoderm cells (Fig. 3R), and the mid- and hindgut degenerate into a cord-like structure (Fig. 3S).

Definitive endoderm is depleted from the lateral region of the embryonic gut of *Sox17*$^{-/-}$ embryos

The histological changes in the epithelium of the embryonic gut point to the deficiency of definitive endoderm during gut development in the *Sox17*$^{-/-}$ embryo. To characterise the cell types present in the gut of the mutant embryo, the expression of definitive endoderm markers was examined by in situ hybridisation studies.

Hnf3α and *Hnf3β* are expressed in the definitive endoderm (Ang et al., 1993; Monaghan et al., 1993; Sasaki and Hogan, 1993), and the activity of both genes is critical for the formation of the definitive endoderm and its derivatives (Ang and Rossant, 1994; Dufort et al., 1998; Duncan et al., 1998; Kaestner et al., 1999). In *Sox17*$^{-/-}$ mutant embryos, *Hnf3α* was expressed in the definitive endoderm at 8.5 and 9.5 dpc (Fig. 4A-D). However, in contrast to the normal (+/+ and +/–) embryos, *Hnf3α*-expressing cells were confined to a much narrower domain in the medial and paraxial region of the embryonic gut along the entire anteroposterior axis of the mutant embryo (Fig. 4A-D). The number of *Hnf3α*-positive cells (per transverse section of the gut of 8.5 dpc embryo, n=4) was significantly reduced (P<0.01) in the endoderm in both the anterior (normal, 40.0±2.1; mutant, 18.0±1.5) and the posterior parts of the embryo (normal, 38.5±3.0; mutant, 20.3±4.2). *Hnf3β* expression was weak in the cells in the degenerating segments but was maintained in the floor plate of the neural tube of the 9.5 dpc mutant embryo (Fig. 4E). *Cdx2*-expressing population (Beck et al., 1995) was also reduced in the hindgut of the mutant embryo (Fig. 4F,G). *Hex*, which is normally expressed in the definitive endoderm (Keng et al., 2000; Martinez Barbera et al., 2000), was expressed in a more restricted domain in the endoderm of the foregut portal (8.5 dpc; Fig. 4H). These findings suggest that the cell population that displays markers of definitive endoderm is significantly reduced in the embryonic gut of the mutant embryo.

Hex is expressed in the liver and thyroid primordia from 9.0 dpc onwards, and is essential for the development of the liver and thyroid (Keng et al., 2000; Martinez Barbera et al., 2000). In *Sox17*$^{-/-}$ mutant embryos, *Hex* was expressed on time in both thyroid and liver primordia (Fig. 4I), which provides additional evidence that the initial development of these foregut derivatives is not affected (Fig. 3Q,R). *Pdx1*, which is necessary for the pancreatic outgrowth and the differentiation of the rostral duodenum (Jonsson et al., 1994; Offield et al., 1996), is expressed in the dorsal and ventral pancreatic regions of the gut endoderm after 8.5 dpc (Guz et al., 1995). In the *Sox17*$^{-/-}$ mutant embryos, *Pdx1* expression was not detected in the gut tissues at the sites of the primordia of either the dorsal or the ventral pancreatic buds (Fig. 4J). Therefore, in contrast to the independence of liver and thyroid on normal *Sox17* function to initiate early differentiation, *Sox17* activity may be essential for the formation of the pancreas.

During gut development, Sonic hedgehog (*Shh*) and Indian hedgehog (*Ihh*) are expressed in the endoderm and play crucial roles in the regionalisation of the primitive gut tube (Apelqvist et al., 1997; Hebrok et al., 1998; Ramalho-Santos et al., 2000; Sukegawa et al., 2000). In the 8.5-9.5 dpc *Sox17* mutants, *Shh* was expressed at a low level in the anterior endoderm (open arrows in Fig. 4L,N,O), but was absent from the posterior endoderm (Fig. 4K,M) and the mid- and hindgut epithelia (Fig. 4N,P). Similarly, *Ihh* expression was absent in the endoderm of the mutant embryonic gut (8.5 dpc; Fig. 4Q) and the mid- and hindgut epithelia (9.5 dpc; Fig. 4R). However, *Ihh* expression in the visceral endoderm was not altered.

Besides the deficiency of the definitive endoderm and abnormal morphogenesis of the mid- and hindgut, no other obvious abnormality was found in other germ-layer derivatives and organs of the *Sox17* mutant embryos, except for the absence of the mesenchymal tissue that normally intercalates between the splanchnic mesothelium and the endoderm in the lateral region of the embryonic gut. *Ptch*, which encodes a receptor that modulates Hedgehog (Hh) signalling (Goodrich et al., 1996; Motoyama et al., 1998), was not expressed in the splanchnic mesothelium (Fig. 4S,T); however, it was expressed appropriately in the floor plate and the ventral part of the paraxial mesoderm. These findings suggest that the disruption of Hh signalling activity revealed by the loss of *Shh* and *Ihh* expression in the endoderm of the embryonic gut and *Ptch* expression in the neighbouring mesothelium may cause the loss of the splanchnic mesenchyme in *Sox17*$^{-/-}$ mutant embryo (Fig. 3O).

Correct tissue- and region-specific expression of several genes was observed in the cranial neural tube [*Otx2* (Simeone et al., 1992); data not shown], somites [*Meox1* (Candia et al., 1992); data not shown], the cardiogenic mesoderm (*Gata4*, Fig. 6F,G), the notochord (*T*, data not shown; *Shh*, Fig. 4K-P) and the tail bud mesenchyme (*T*, *Wnt3α* and *Wnt5a*, data not shown; *Cdx2*, Fig. 4F) of the mutant embryos before any disruption of the trunk and tail morphology became evident.

Loss of *Sox17* function elevates apoptosis but does not affect the formation of anterior definitive endoderm

The histological and in situ hybridisation analyses

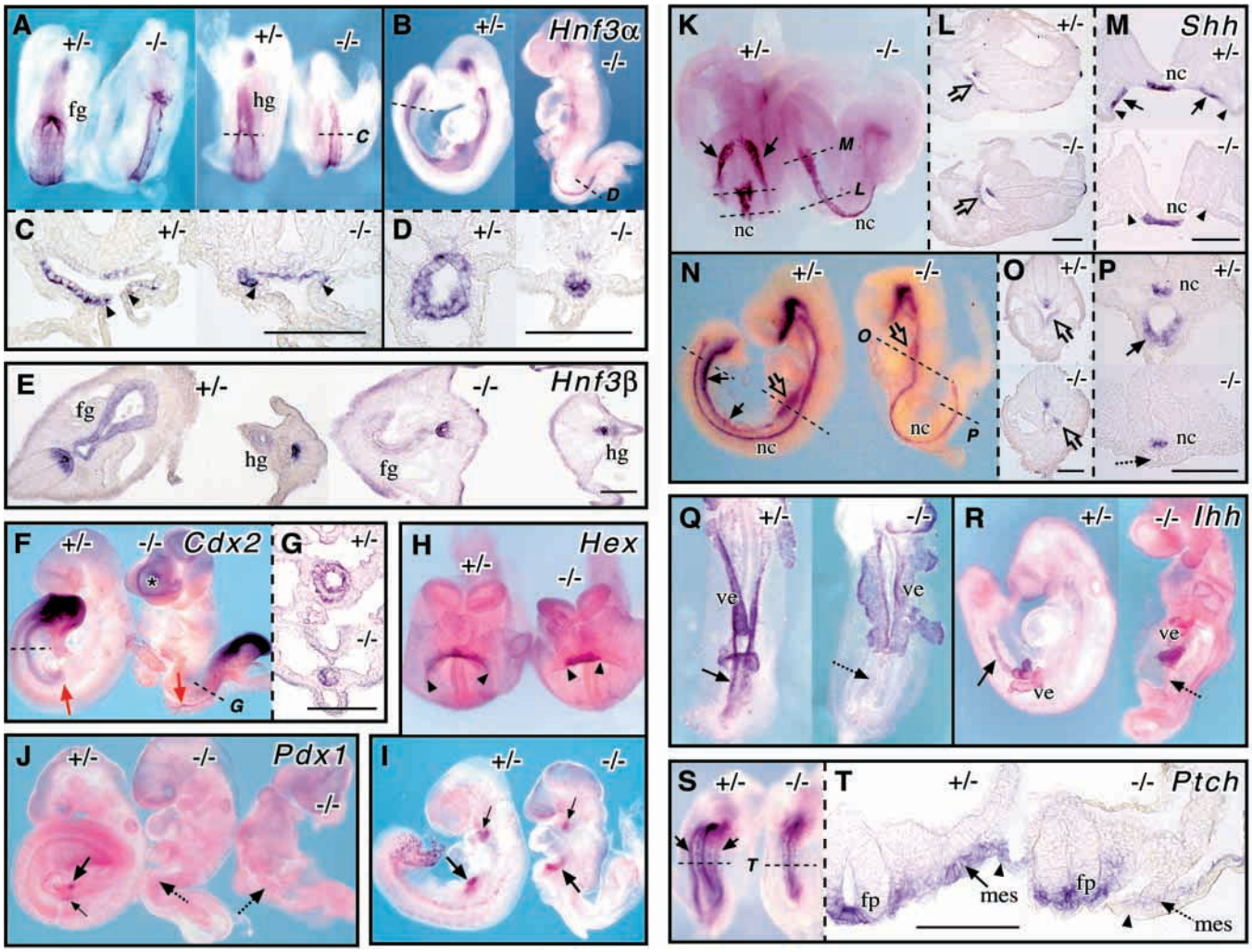

Fig. 4. Depletion of the definitive gut endoderm in *Sox17*$^{-/-}$ embryos. (A-D) *Hnf3α* expression in the definitive gut endoderm of the 8.5 (A,C) and 9.5 (B,D) dpc normal and mutant embryos [A includes both anterior (left) and posterior (right) views of the same embryos]. *Hnf3α* expressing cells are confined to a much narrower medial and paraxial domain in the embryonic gut of the mutant embryo. (E) Transverse sections of 9.5 dpc embryos demonstrate normal *Hnf3β* expression pattern in the reduced hindgut endoderm and the floor plate of the heterozygous (+/–) and null mutant (–/–) embryos. (F,G) 9.5 dpc mutant (–/–) embryos showing normal *Cdx2* expression in the endoderm of the gut posterior to the level marked by the red arrow (F, lateral view; G, transverse section at the plane indicated by the broken line in F). (H,I) *Hex* expression in the foregut endoderm of 8.5 dpc embryos (H; anterior view) and in the thyroid (small arrows) and liver (large arrows) buds of 9.5 dpc embryos (I; lateral view). (J) *Pdx1* expression in dorsal (small arrow) and ventral (large arrow) pancreatic regions of the gut endoderm in 9.5 dpc heterozygous embryos (left-most in the figure). *Pdx1* expression is completely absent (broken arrows) in the prospective pancreatic tissues of the homozygous (–/–) mutant embryos (two on the right hand side). (K-P) *Shh* expression in the definitive gut endoderm (open arrows for foregut, solid arrows for mid to hindgut) and notochord of 8.5 (K, posterior view; L,M, transverse sections) and 9.5 dpc embryos (N, lateral view; O,P, transverse sections). In plate P, the broken arrow shows the *Shh*-negative posterior gut in the mutant (–/–) embryo. (Q,R) *Ihh* expression in the visceral and definitive endoderm of 8.5 (Q; ventral view) and 9.5 (R; lateral view) dpc embryos. The unbroken arrows indicate the *Ihh*-positive endoderm in the heterozygous embryo and the broken arrows indicate the absence of *Ihh* expression in the equivalent endodermal tissues in the homozygous mutant embryo. (S,T) *Ptch* expression in the ventral structures of the 8.5 dpc mutant embryos (S, ventral view; T, transverse section). The unbroken arrows indicate the *Ptch*-positive splanchnic mesothelium in the heterozygous embryo and the broken arrows indicate the absence of *Ptch* expression in the equivalent tissues in the homozygous mutant embryo. Broken lines on the whole-mount figures show the plane of histological sections. Arrowheads in C,H,M,T indicate the border between the presumptive visceral endoderm and the definitive endoderm. fg, foregut; fp, floor plate; hg, hindgut; nc, notochord; mes, mesothelium; ve, visceral endoderm; asterisk, nonspecific signals that are due to antibody trapping in lumen. Scale bars: 100 μm.

demonstrated that the loss of *Sox17* activity causes the depletion of the definitive endoderm in the embryonic gut. The occurrence of apoptosis of the endoderm of the *Sox17*$^{-/-}$ mutant was examined by TUNEL analysis. Mutant embryos did not show any more TUNEL-positive cells than the normal embryos prior to the neural plate stage (Fig. 5A). There was, however, a significant increase of the number of TUNEL-positive cells in the prospective foregut endoderm underneath the anterior and lateral margin of the neural plate by the late neural plate to early headfold stages (Fig. 5B,D-F), but no

appreciable increase of apoptotic cell death was found in the posterior definitive endoderm (Fig. 5C,D). Apoptotic cells were found more frequently in the endoderm in the medial region of the prospective foregut of the mutant embryo (Fig. 5G-I; normal, 0.33±0.17; mutant; 1.13±0.23; *n*=4). Interestingly, in the mutant embryo, normal *Cer1* expression was found in the prospective foregut endoderm at the early-bud to headfold stages (Shawlot et al., 1998) (Fig. 5J,K). This suggests that the initial formation of the anterior definitive endoderm is therefore not affected by the loss of *Sox17* activity, but increased cell death may underpin the deficiency of endoderm in the foregut. By contrast, there was no significant increase in the number of TUNEL-positive cells in the prospective hindgut of the mutant embryo (Fig. 5H; normal, 0.13±0.11; mutant, 0.14±0.12; *n*=4). The depletion of the definitive endoderm in the posterior segment of the embryonic gut may be caused by factors other than apoptosis.

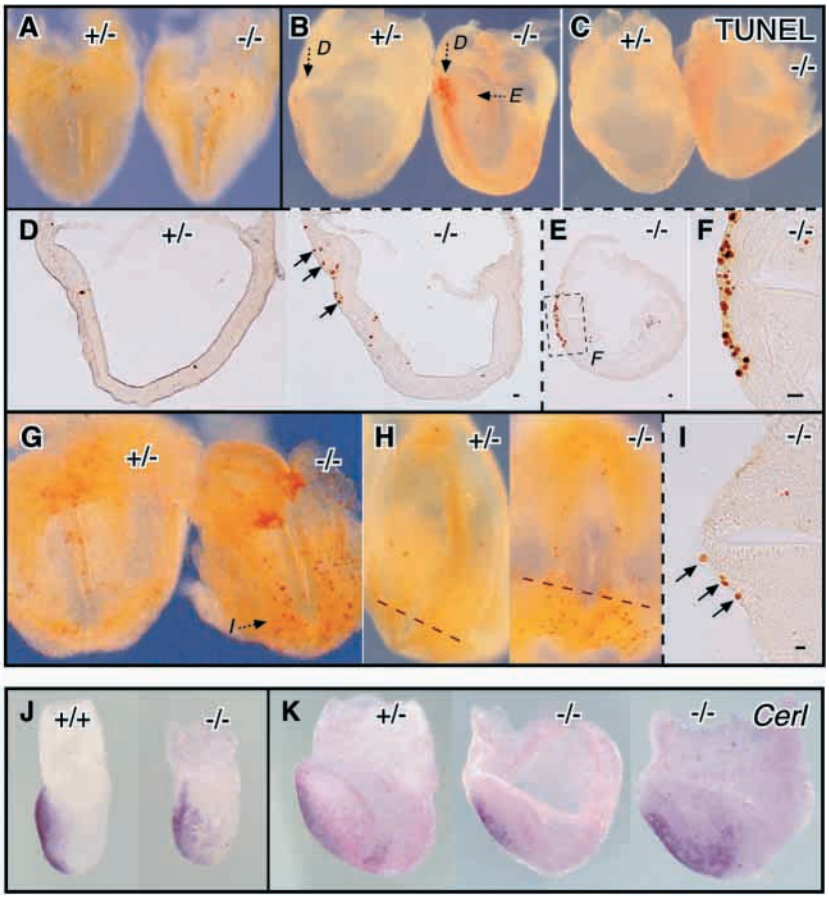

Fig. 5. Loss of *Sox17* function elevates apoptosis but does not affect the initial formation of anterior definitive endoderm. (A-I) Whole-mount TUNEL staining (brown) of the mutant embryos at early neural plate (A, anterior view), late neural-plate to early head-fold [anterolateral (B), posterior (C), sagittal section (D) and transverse sections (E,F)] and early somite stages [anterior (G), posteroventral (H) and transverse section (I)]. Mutant embryos do not show any more TUNEL-positive cells than do the normal (+/+ and +/–) embryos prior to the neural plate stage (A). However, at the late neural plate to early somite stages, more TUNEL-positive cells are found in the prospective foregut endoderm (B,E-G; arrows in D,I). By contrast, no increase in apoptosis is found in the posterior endoderm (C,D,H). In H, the broken red lines indicate the border between anterior and posterior gut segments. The broken arrows in B,G show the plane of sectioning (D,E,I); the broken rectangle (E) marks the area shown in the magnified view (F). (J,K) *Cer1* expression in the anterior definitive endoderm of the normal and mutant embryos at early- to late-bud stage (J, lateral view) and at late neural-plate stage (K, lateral view). Proper expression of *Cer1* was found in the prospective foregut endoderm of the normal (+/+ and +/–) and null mutant embryos. Scale bars: 10 μm.

Visceral endoderm replaces definitive endoderm in the lateral region of the embryonic gut

The visceral endoderm of the yolk sac characteristically displays active endocytosis, revealed by the uptake of horseradish peroxidase (HRP) for transporting macromolecules across the foetal membrane (Bielinska et al., 1999). The visceral endoderm in the yolk sac of the mutant embryos showed normal HRP-uptake activity (Fig. 6A-C). However, endodermal cells that actively incorporate HRP are also found in the prospective gut region of the embryo at late headfold to early somite stage, resulting in a significant reduction in the area of non-HRP-labelled definitive endoderm that is confined to the paraxial and medial region of the embryonic gut. Several genes that are expressed in the visceral endoderm [*Hnf4* (Chen et al., 1994); *Gata4* (Molkentin et al., 1997; Narita et al., 1997); *Ihh* (Maye et al., 2000)] also show an increase in their expression domain into the lateral region of the gut of the mutant embryo (*Hnf4*, Fig. 6D,E; *Gata4*, Fig. 6F,G; *Ihh*, Fig. 4Q). α-Fetoprotein (*Afp*), which is expressed specifically in the extra-embryonic part of the visceral endoderm (Dziadek and Adamson, 1978), restricts its expression to the visceral endoderm up to the early neural plate stage (Fig. 6H) but extends into the posterior and lateral regions of the embryonic gut of the headfold stage mutant embryo (Fig. 6I,J). By contrast, no significant expansion of *Afp* expression domain was found in the anterior region of the embryonic gut at this stage of development (Fig. 6I).

Our results show that deficiency in the definitive endoderm in different region of the embryonic gut may be brought about differently by apoptosis and inadequate population expansion during the neural-plate to headfold stages. The expansion of the visceral endoderm-like cells into the embryonic gut and the loss of the expression of markers for definitive endoderm all suggest that the reduced population of definitive endoderm could not effectively displace the visceral endoderm to the extra-embryonic sites and results in the occupation of the substantial region of the gut by an inappropriate type of cells.

Sox17 acts cell autonomously to bestow endodermal potency

To assess the impact of the loss of *Sox17* on tissue potency, the differentiation of *Sox17* mutant cells was examined in chimaeric mouse embryos comprised of $Sox17^{-/-}$ ES cells and blastocyst derived from ROSA26 ($Sox17^{+/+}$) mice which constitutively express β-galactosidase (Tremblay et al., 2000).

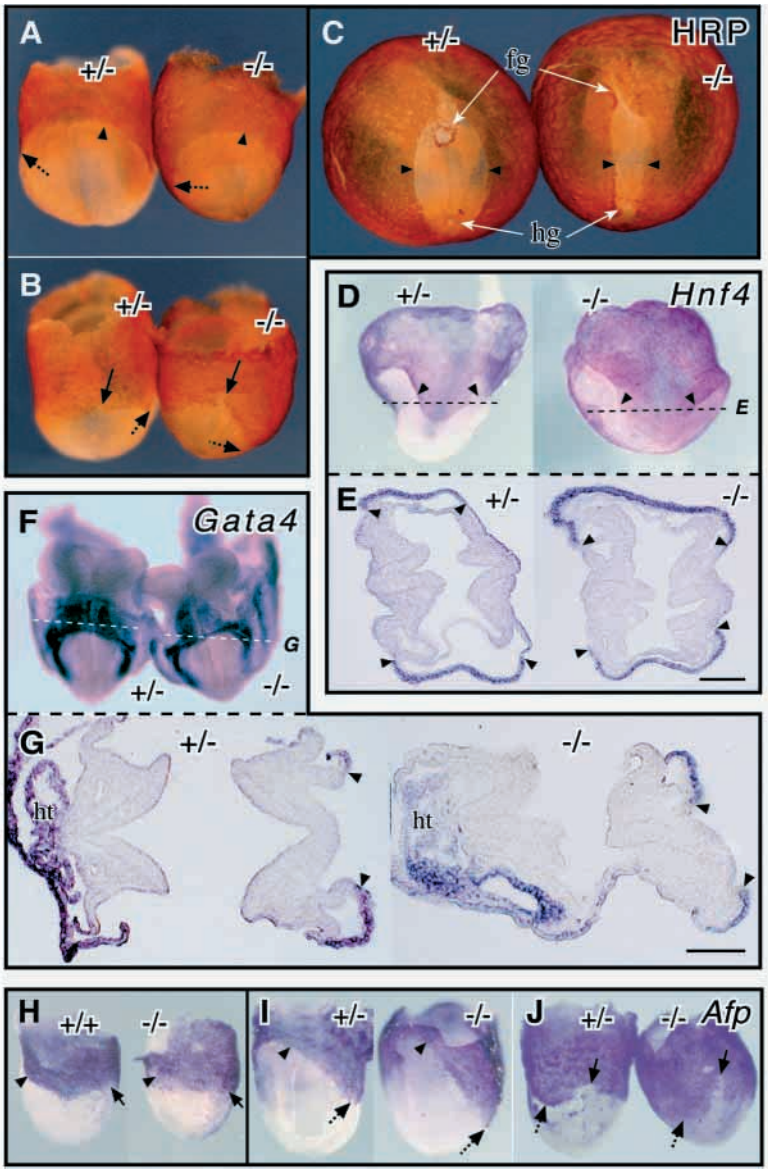

Fig. 6. Visceral endoderm replaces the definitive endoderm in the lateral region of the embryonic gut. (A-C) The 8.0 dpc [late headfold stage; anterior (A) and posterior (B) views of the same embryos] and 8.5 dpc (C, ventral view) mutant embryos showing the endocytotic activity of visceral endoderm revealed by the uptake of horseradish peroxidase (HRP; 2 mg/ml, brown staining reaction) for 30 minutes. The visceral endoderm in the yolk sac of the mutant embryos demonstrate normal HRP-uptake activity, but the endodermal cells displaying similar uptake activity are also found in the prospective gut region of the embryo (A,B, broken arrows; C, arrowheads). (D,E) Expression of *Hnf4* in the visceral endoderm of the 8.5 dpc mutant embryos (D, lateral view; E, transverse section), reveals the expansion of the *Hnf4* expression domain into the lateral region of both anterior and posterior gut in the mutant embryo (arrowheads). (F,G) Expression of *Gata4* in the cardiogenic mesoderm (ht) and visceral endoderm (F, anterior view; G, transverse section) of the 8.5 dpc mutant embryos. *Gata4* expression, which is normally restricted to the visceral endoderm, extends into the lateral regions of the posterior gut in the mutant embryos (G, arrowheads). (H-J) *Afp* expression in the visceral endoderm of the normal and mutant embryos at early neural plate (H, lateral view) and headfold stages [anterolateral (I) and posterior (J) views of the same embryos]. In the mutant embryos, *Afp* expression is associated with the yolk sac endoderm until the early neural plate stage (H), but by the headfold stage, expression extends into the posterior and lateral regions of the embryonic gut (I,J, broken arrows). In A,B,H-J, the anterior, lateral and posterior border between visceral and definitive endoderm is indicated by arrowheads, broken arrows and arrows, respectively. In C-E,G, arrowheads mark the border between the visceral endoderm and the definitive endoderm. The broken lines in D and F mark the plane of sectioning. fg, foregut; hg, hindgut; ht, heart. Scale bar: 100 μm.

Twelve of the 31 chimaeric embryos harvested at 8.25 and 9.5 dpc showed more than 80% tissue contribution by *Sox17*$^{-/-}$ ES cells. Five chimeras (one at 8.25 dpc and four at 9.5 dpc) with high mutant ES cell contribution displayed a reduction in embryonic gut size and failed to undergo axis rotation (Fig. 7A-D,E,F), which recapitulates the phenotype of the *Sox17*-null mutant embryos. The remaining seven chimaeric (seven at 9.5 dpc) embryos, containing moderate to high mutant ES cell contribution, were slightly retarded (Fig. 7E; one showed delayed axis rotation) but were otherwise morphologically normal.

Histological analysis of the chimaeric embryos showed that the *Sox17*$^{-/-}$ ES cells can contribute extensively to the ectodermal and mesodermal tissues (such as skin, neural tube, notochord, somites, lateral plate mesoderm and yolk sac mesoderm; Fig. 7B-D,F-K). Of significant interest, however, is the marked reduction in the contribution by mutant ES cells to the foregut endoderm (Fig. 7B,C,H,I) and the almost complete exclusion of the mutant cells from the mid- and hindgut endoderm (Fig. 7D,F,J,K). This finding clearly points to the cell-autonomous activity of *Sox17* in regulating differentiation of the definitive endoderm particularly in the mid- and hindgut of the embryo. The differential impact of the loss of *Sox17* function on the endodermal potency of cells colonising the foregut versus those colonising the mid- and hindgut underpins the different defects between the anterior and posterior endoderm formation in the null mutant embryos. In the chimeras, only the wild-type host cells contributed to the extra-embryonic visceral endoderm. That the restoration of *Sox17* activity in the visceral endoderm has neither enhanced nor rescued the morphological abnormality and the depletion of definitive endoderm displayed by the chimeras with the strongest mutant ES cell contribution indicates that *Sox17* function in the extra-embryonic tissues is not crucial for embryogenesis. The phenotype of the null mutant embryo is therefore primarily caused by the defective differentiation of the derivatives of the *Sox17*-deficient epiblast.

DISCUSSION

A critical role of Sox17 in the differentiation of the definitive endoderm in the mouse

The findings of the phenotypic analysis of the *Sox17*-null mutant embryo show that *Sox17* plays a crucial role in the

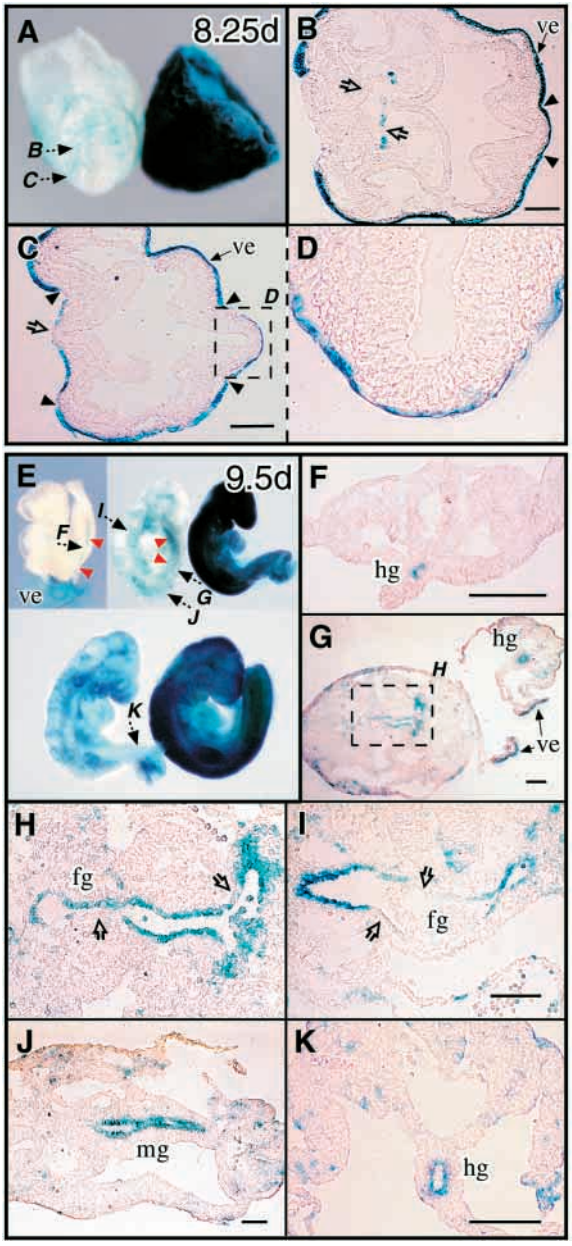

Fig. 7. The lack of contribution of *Sox17*$^{-/-}$ ES cells in the gut endoderm in the chimera. ROSA26-derived cells are positive for X-gal staining (blue staining), while the ES clone (*Sox17*$^{-/-}$)-derived cells are negative. (A,E) Whole mount view of chimaeric embryos with the high contribution of *Sox17*$^{-/-}$ ES cells and non-chimaeric littermates (right) at 8.25 (A) and 9.5 (E) dpc. (E) Three chimeras with various degrees of mutant ES cell contribution: one chimera with high mutant ES cell contribution displays no axis rotation (upper left), while two other chimeras containing moderately high mutant ES cell contribution are slightly retarded in posterior trunk development [one shows delayed axis rotation (lower left)]. The broken arrows show the plane of the sectioning image in the designated plate. In E, red arrowheads show the posterior gut endoderm, which was composed mostly of the ROSA26 (*Sox17*$^{+/+}$) host-derived cells. (B-D,F-K) Transverse sections of chimaeric embryos at 8.25 (B-D) and 9.5 (F-K) dpc. *Sox17*$^{-/-}$ ES cells were excluded from the posterior or mid- and hindgut endoderm, which is mainly composed of ROSA26 host-derived cells (B-D,F,G,J,K). *Sox17*$^{-/-}$ mutant cells can contribute to the anterior or foregut endoderm (open arrows in B,C,H,I). The chimeras with the high mutant ES cell contribution display a reduction in cell population of the posterior definitive endoderm (B,C) or embryonic gut (F). Arrowheads show the border between visceral endoderm and definitive endoderm. The broken rectangle encompasses the area magnified in the designated plate. fg, foregut; hg, hindgut; mg, midgut; ve, visceral endoderm. Scale bars: 100 μm.

maintenance and differentiation of the definitive endoderm of the embryonic gut. *Sox17* function may not be essential for the formation of the progenitor cells of the definitive endoderm during gastrulation but is required for sustaining the viability of the foregut endoderm and the elaboration of the mid- and hindgut endoderm. The loss of *Sox17* function results in the apoptosis of the endoderm in the foregut and the failure of the expansion of the endoderm of the mid- and hindgut. The diminished contribution of *Sox17*$^{-/-}$ mutant cells to the gut endoderm of the chimera further shows that *Sox17* is essential for the embryonic cells to acquire an endodermal potency.

The lack of defects in the development of the extra-embryonic endoderm and the initial phase of the formation of anterior definitive endoderm in *Sox17* mutant raise the possibility of potential redundancy of other gene activity. Members of the Sox gene family share similar DNA-binding specificity, especially within the same subgroup. Among the members, *Sox7*, *Sox17* and *Sox18*, of mammalian Sox subgroup F, *Sox18* has been shown to be expressed in yolk-sac blood islands, the developing endothelial cells and presumptive endocardial cells, but not in the endoderm cell lineage during early embryogenesis (Pennisi et al., 2000). Analyses of expression revealed that *Sox7* and *Sox17* genes are co-expressed in the extra-embryonic visceral endoderm, suggesting that there may be functional compensation by *Sox7*, which could account for the lack of discernible defects on the visceral endoderm in the *Sox17*-null mutant embryo. However, only *Sox17* is expressed in the definitive gut endoderm, suggesting redundancy among the subgroup F members is unlikely in the definitive endoderm lineage. The severity of the posterior gut phenotype of the *Sox17* mutant further implicate that although *Sox2* is expressed throughout the gut endoderm, and *Sox3* transcripts are also detected in the posterior region of the foregut in mouse early-somite stage embryos (Wood and Episkopou, 1999), the activity of these two Sox genes are not sufficient to compensate for the loss of *Sox17* function. Recently, the *casanova* mutation, which causes defective endoderm formation in the zebrafish, has been found to involve a novel *Sox* gene of the subgroup F (Dickmeis et al., 2001; Kikuchi et al., 2001; Sakaguchi et al., 2001). Whether any *casanova* orthologue is present in the higher vertebrates is unclear.

A possible morphogenetic role of the *Sox17*-expressing definitive endoderm

During early embryogenesis, morphogenetic activity of the extra-embryonic visceral endoderm has been shown to be important in the establishment of the body plan of the embryo (Beddington and Robertson, 1998; Beddington and Robertson, 1999; Brennan et al., 2001; Episkopou et al., 2001; Hoodless et al., 2001; Kalantry et al., 2001; Lu et al., 2001; Yamamoto et al., 2001). Despite the expression of *Sox17* in the extra-embryonic visceral endoderm of the embryo during

gastrulation and early organogenesis, no early developmental defects are found in the *Sox17* mutant embryo. The overlapping expression of the structurally homologous *Sox7* may have provided the redundancy that functionally compensates for the loss of *Sox17* activity. The defective differentiation of the definitive endoderm in the mutant embryo suggests that similar functional overlap of the activity of other Sox genes of the same subgroup or any other endoderm-specific genes are absent. However, the disorganised development of the posterior trunk and the interruption of axis morphogenesis may point to some secondary impact of either the loss of *Sox17* function in the definitive endoderm or the abnormal formation of the embryonic gut that is deficient of the proper type of endodermal cells.

Several studies have suggested that the definitive endoderm may exert morphogenetic influence on the development of the mesoderm and ectodermal tissues. The anterior definitive endoderm and Hex activity specifically expressed in this tissue are required in tissues for normal forebrain formation (Martinez Barbera et al., 2000; Withington et al., 2001). In the *Sox17*$^{-/-}$ mutant embryo, proper though spatially restricted, the expression of several genes such as *Hnf3α*, *Hnf3β*, *Hex*, *Cer1* and *Cdx2* is still present in the endoderm of the embryonic gut. This may suggest that whatever morphogenetic activity exerted by the definitive endoderm is still provided to other germ-layer derivatives before extensive loss of anterior definitive endoderm by apoptosis occurs. This may account for the apparently normal development of the cranial and upper trunk structures. Development of the more posterior trunk structures is becoming more severely affected with more extensive depletion of the definitive endoderm in the posterior segments of the embryonic gut. In this regard, the loss of *Shh* and *Ihh* activity in the endoderm and the concurrent downregulation of *Ptch* expression in the lateral plate mesoderm may be significant. Whether the specific loss of Hh signalling in the gut endoderm but not in other structures such as the notochord and the floor plate is associated with the retarded development and growth of posterior trunk structures of the *Sox17*$^{-/-}$ embryos is still unclear. However, a more widespread deficiency in Hh signalling in the *Shh*/*Ihh*-double mutant embryo has also resulted in a similar developmental arrest phenotype with the lack of axis rotation at the early somite stage (Zhang et al., 2001). Consistent with this notion, Hh signalling has been shown to play a crucial role in the regionalisation of the primitive gut tube by acting through the adjacent mesoderm (Apelqvist et al., 1997; Hebrok et al., 1998; Ramalho-Santos et al., 2000; Sukegawa et al., 2000).

Different impact of the loss of *Sox17* activity on the anterior and posterior definitive endoderm

Results of the chimera study reveal that the *Sox17*$^{-/-}$ mutant ES cells are less competent to colonise the foregut endoderm and are excluded from the mid- and hindgut. In the null mutant embryo, *Sox17*-deficient cells can form the early endodermal progenitor and can contribute to the definitive endoderm in all regions of the gut. However, increased apoptosis of the mutant cells in the foregut and failure of mutant cells to differentiate or proliferate in the posterior gut leads to the depletion of the definitive endoderm in all segments of the embryonic gut. These findings strongly suggest that *Sox17* may function differentially as a maintenance factor in the endoderm of the foregut and a differentiation regulator in the rest of the embryonic gut.

The different impact of the loss of *Sox17* function on the potency of the cells to contribute to different parts of the gut of the chimera points to a variable requirement for *Sox17* activity in the allocation of different populations of definitive endoderm. Like the *Sox17* mutant cells, *Smad2*-deficient cells are able to contribute at a moderate level to the anterior definitive endoderm, but are absent from the hindgut (Tremblay et al., 2000). While *Sox17*-deficient cells are unable to colonise the mid- and hindgut of the chimera, *Hnf3β*-deficient cells can form the hindgut, but are not in the foregut and midgut, of chimeras generated from the null ES cells and the tetraploid embryo (Dufort et al., 1998). These findings strongly suggest a differential requirement of *Sox17*, *Smad2* and *Hnf3β* in the endoderm of different parts of the embryonic gut. The similarity in behaviour of the *Sox17*- and *Smad2*-deficient cells in the chimera is consistent with the recent demonstration that *Xsox17* activity may be required for the maintenance of Nodal signalling activity in the cells that are primed for endodermal differentiation in the *Xenopus* (Engleka et al., 2001; Aoki et al., 2002).

Evolutionary conservation of molecular pathways in endoderm formation among vertebrates

In the *Xenopus*, *Xsox17α* and *Xsox17β* direct the differentiation of embryonic cells towards the endodermal fate in a cell-autonomous fashion (Hudson et al., 1997; Clements and Woodland, 2000). Furthermore, the activation of *Xsox17* by VegT enables the delineation of the endodermal progenitor from other germ-layer tissues and initiates endoderm differentiation (Engleka et al., 2001). Recently, the isolation and characterisation of other genes involved with endoderm formation in *Xenopus* and zebrafish has enabled the construction of a molecular pathway involving nodal-related signalling and the induction of Mix-type homeobox or Gata-type zinc-finger genes, which in turn activate the endoderm determining genes, *Sox17* and *Hnf3β* (Alexander and Stainier, 1999; Reiter et al., 2001). In mouse early embryogenesis, *Hnf3β* (Dufort et al., 1998), *Gata4* (Narita et al., 1997), *Smad2* (Tremblay et al., 2000) and *Fast1* (Hoodless et al., 2001), which are involved in Activin/Nodal-related signalling, play an important role in the formation of the definitive endoderm. The phenotypic consequences of the loss of *Sox17* function in the mouse are consistent with the concept that *Sox17* activity is required by the progenitor cells to acquire endodermal potency and to differentiate properly into definitive endoderm. Our findings highlight the conservation of *Sox17* function in endoderm formation during vertebrate embryogenesis.

The authors thank Drs P. Koopman, H. Hamada, T Hara and Y. Saijoh for their kind and helpful advice and discussion regarding this work and their critical reading of this paper. They also thank Dr N. Fujisawa for his generous assistance, and Mr I. Tsugiyama and Mrs H. Hayashi for their technical and secretarial support. The authors are grateful to Drs E. Olson, A. McMahon, B. G. Herrmann, C. V. Wright, H. Hamada, I. Matsuo, S.-L. Ang, J. Motoyama, H. Sasaki, Y. Hiraoka, J. Barras, S. Dunn, T. Noguchi, F. Guillemot, D. Anderson and M. Wilkinson for providing the in situ probes. This work was mainly supported by financial grants from the Ministry of Education, Science, Sports and Culture of Japan to Y. Kanai (numbers 11660306 and 13660295). This work was also supported by the Program for

Promotion of Basic Research Activities for Innovative Biosciences (Y. K.), the Sumitomo Foundation (M. K.-A.), the National Health and Medical Research Council (NHMRC) of Australia and Mr James Fairfax (P. P. L. T., J. M. G.). P. P. L. T. is a NMHRC Senior Principal Research Fellow. This paper is dedicated to the memory of Dr Toshiya Yamada (Institute for Molecular Bioscience, The University of Queensland, Australia), our dear friend, who died on 12th May 2001.

REFERENCES

Alexander, J. and Stainier, D. Y. (1999). A molecular pathway leading to endoderm formation in zebrafish. *Curr. Biol.* **9**, 1147-1157.

Ang, S. L. and Rossant, J. (1994). HNF-3 beta is essential for node and notochord formation in mouse development. *Cell* **78**, 561-574.

Ang, S. L., Wierda, A., Wong, D., Stevens, K. A., Cascio, S., Rossant, J. and Zaret, K. S. (1993). The formation and maintenance of the definitive endoderm lineagein the mouse: involvement of HNF3/forkhead proteins. *Development* **119**, 1301-1315.

Aoki, T. O., David, N. B., Minchiotti, G., Saint-Etienne, L., Dickmeis, T., Persico, G. M., Strähle, U., Mourrain, P. and Rosa, F. M. (2002). Molecular integration of *casanova* in the Nodal signalling pathway controlling endoderm formation. *Development* **129**, 275-286

Apelqvist, A., Ahlgren, U. and Edlund, H. (1997). Sonic hedgehog directs specialised mesoderm differentiation in the intestine and pancreas. *Curr. Biol.* **7**, 801-804.

Beck, F., Erler, T., Russell, A. and James, R. (1995). Expression of *Cdx-2* in the mouse embryo and placenta: possible role in patterning of the extra-embryonic membranes. *Dev. Dyn.* **204**, 219-227.

Beddington, R. S. and Robertson, E. J. (1998). Anterior patterning in mouse. *Trends Genet.* **14**, 277-284.

Beddington, R. S. and Robertson, E. J. (1999). Axis development and early asymmetry in mammals. *Cell* **96**, 195-209.

Bi, W., Deng, J. M., Zhang, Z., Behringer, R. R. and de Crombrugghe, B. (1999). *Sox9* is required for cartilage formation. *Nat. Genet.* **22**, 85-89.

Bielinska, M., Narita, N. and Wilson, D. B. (1999). Distinct roles for visceral endoderm during embryonic mouse development. *Int. J. Dev. Biol.* **43**, 183-205.

Bishop, C. E., Whitworth, D. J., Qin, Y., Agoulnik, A. I., Agoulnik, I. U., Harrison, W. R., Behringer, R. R. and Overbeek, P. A. (2000). A transgenic insertion upstream of *Sox9* is associated with dominant XX sex reversal in the mouse. *Nat. Genet.* **26**, 490-494.

Bowles, J., Schepers, G. and Koopman, P. (2000). Phylogeny of the SOX family of developmental transcription factors based on sequence and structural indicators. *Dev. Biol.* **227**, 239-255.

Brennan, J., Lu, C. C., Norris, D. P., Rodriguez, T. A., Beddington, R. S. and Robertson, E. J. (2001). Nodal signalling in the epiblast patterns the early mouse embryo. *Nature* **411**, 965-969.

Candia, A. F., Hu, J., Crosby, J., Lalley, P. A., Noden, D., Nadeau, J. H. and Wright, C. V. (1992). *Mox-1* and *Mox-2* define a novel homeobox gene subfamily and are differentially expressed during early mesodermal patterning in mouse embryos. *Development* **116**, 1123-1136.

Chen, W. S., Manova, K., Weinstein, D. C., Duncan, S. A., Plump, A. S., Prezioso, V. R., Bachvarova, R. F. and Darnell, J. E. J. (1994). Disruption of the *HNF-4* gene, expressed in visceral endoderm, leads to cell death in embryonic ectoderm and impaired gastrulation of mouse embryos. *Genes Dev.* **8**, 2466-2477.

Clements, D. and Woodland, H. R. (2000). Changes in embryonic cell fate produced by expression of an endodermal transcription factor, Xsox17. *Mech. Dev.* **99**, 65-70.

Constam, D. B. and Robertson, E. J. (2000). Tissue-specific requirements for the proprotein convertase furin/SPC1 during embryonic turning and heart looping. *Development* **127**, 245-254.

Deng, C. X., Wynshaw-Boris, A., Shen, M. M., Daugherty, C., Ornitz, D. M. and Leder, P. (1994). Murine FGFR-1 is required for early postimplantation growth and axial organization. *Genes Dev.* **8**, 3045-3057.

Dickmeis, T., Mourrain, P., Saint-Etienne, L., Fischer, N., Aanstad, P., Clark, M., Strahle, U. and Rosa, F. (2001). A crucial component of the endoderm formation pathway, *CASANOVA*, is encoded by a novel sox-related gene. *Genes Dev.* **15**, 1487-1492.

Dufort, D., Schwartz, L., Harpal, K. and Rossant, J. (1998). The transcription factor HNF3beta is required in visceral endoderm for normal primitive streak morphogenesis. *Development* **125**, 3015-3025.

Duncan, S. A., Navas, M. A., Dufort, D., Rossant, J. and Stoffel, M. (1998). Regulation of a transcription factor network required for differentiation and metabolism. *Science* **281**, 692-695.

Dunn, T. L., Mynett-Johnson, L., Wright, E. M., Hosking, B. M., Koopman, P. A. and Muscat, G. E. (1995). Sequence and expression of *Sox-18* encoding a new HMG-box transcription factor. *Gene* **161**, 223-225.

Dziadek, M. and Adamson, E. (1978). Localization and synthesis of alphafoetoprotein in post-implantation mouse embryos. *J. Embryol. Exp. Morphol.* **43**, 289-313.

Echelard, Y., Epstein, D. J., St-Jacques, B., Shen, L., Mohler, J., McMahon, J. A. and McMahon, A. P. (1993). Sonic hedgehog, a member of a family of putative signaling molecules, is implicated in the regulation of CNS polarity. *Cell* **75**, 1417-1430.

Engleka, M. J., Craig, E. J. and Kessler, D. S. (2001). Vegt activation of *sox17* at the midblastula transition alters the response to nodal signals in the vegetal endoderm domain. *Dev. Biol.* **237**, 159-172.

Episkopou, V., Arkell, R., Timmons, P. M., Walsh, J. J., Andrew, R. L. and Swan, D. (2001). Induction of the mammalian node requires *Arkadia* function in the extraembryonic lineages. *Nature* **410**, 825-830.

Foster, J. W., Dominguez-Steglich, M. A., Guioli, S., Kwok, C., Weller, P. A., Weissenbach, J., Mansour, S., Young, I. D., Goodfellow, P. N., Brook, J. D. and Schafer, A. J. (1994). Campomelic dysplasia and autosomal sex reversal caused by mutations in an *SRY*-related gene. *Nature* **372**, 525-530.

Gad, J. M., Keeling, S. L., Wilks, A. F., Tan, S. S. and Cooper, H. M. (1997). The expression patterns of guidance receptors, DCC and Neogenin, are spatially and temporally distinct throughout mouse embryogenesis. *Dev. Biol.* **192**, 258-273.

Goodrich, L. V., Johnson, R. L., Milenkovic, L., McMahon, J. A. and Scott, M. P. (1996). Conservation of the hedgehog/patched signaling pathway from flies to mice: induction of a mouse patched gene by Hedgehog. *Genes. Dev.* **10**, 301-312.

Guz, Y., Montminy, M. R., Stein, R., Leonard, J., Gamer, L. W., Wright, C. V. and Teitelman, G. (1995) Expression of murine STF-1, a putative insulin gene transcription factor, in beta cells of pancreas, duodenal epithelium and pancreatic exocrine and endocrine progenitors during ontogeny. *Development* **121**, 11-18.

Hebrok, M., Kim, S. K. and Melton, D. A. (1998). Notochord repression of endodermal Sonic hedgehog permits pancreas development. *Genes Dev.* **12**, 1705-1713.

Henry, G. L. and Melton, D. A. (1998). *Mixer*, a homeobox gene required for endoderm development. *Science* **281**, 91-96.

Hoodless, P. A., Pye, M., Chazaud, C., Labbe, E., Attisano, L., Rossant, J. and Wrana, J. L. (2001). FoxH1 (Fast) functions to specify the anterior primitive streak in the mouse. *Genes Dev.* **15**, 1257-1271.

Hudson, C., Clements, D., Friday, R. V., Stott, D. and Woodland, H. R. (1997). Xsox17 alpha and beta mediate endoderm formation in Xenopus. *Cell* **91**, 397-405.

Jonsson, J., Carlsson, L., Edlund, T. and Edlund, H. (1994). Insulin-promoter-factor 1 is required for pancreas development in mice. *Nature* **371**, 606-609.

Kaestner, K. H., Katz, J., Liu, Y., Drucker, D. J. and Schutz, G. (1999). Inactivation of the winged helix transcription factor HNF3alpha affects glucose homeostasis and islet glucagon gene expression in vivo. *Genes Dev.* **13**, 495-504.

Kalantry, S., Manning, S., Haub, O., Tomihara-Newberger, C., Lee, H. G., Fangman, J., Disteche, C. M., Manova, K. and Lacy, E. (2001). The amnionless gene, essential for mouse gastrulation, encodes a visceral-endoderm-specific protein with an extracellular cysteine-rich domain. *Nat. Genet.* **27**, 412-416.

Kamachi, Y., Uchikawa, M., Collignon, J., Lovell-Badge, R. and Kondoh, H. (1998). Involvement of Sox1, 2 and 3 in the early and subsequent molecular events of lens induction. *Development* **125**, 2521-2532.

Kanai, Y., Kanai-Azuma, M., Noce, T., Saido, T. C., Shiroishi, T., Hayashi, Y. and Yazaki, K. (1996). Identification of two *Sox17* messenger RNA isoforms, with and without the high mobility group box region, and their differential expression in mouse spermatogenesis. *J. Cell Biol.* **133**, 667-681.

Kanai-Azuma, M., Kanai, Y., Okamoto, M., Hayashi, Y., Yonekawa, H. and Yazaki, K. (1999). *Nrk*: a murine X-linked NIK (Nck-interacting kinase)-related kinase gene expressed in skeletal muscle. *Mech. Dev.* **89**, 155-159.

Keng, V. W., Yagi, H., Ikawa, M., Nagano, T., Myint, Z., Yamada, K., Tanaka, T., Sato, A., Muramatsu, I., Okabe, M., Sato, M. and Noguchi, T. (2000). Homeobox gene *Hex* is essential for onset of mouse embryonic

liver development and differentiation of the monocyte lineage. *Biochem. Biophys. Res. Commun.* **276**, 1155-1161.

Kikuchi, Y., Agathon, A., Alexander, J., Thisse, C., Waldron, S., Yelon, D., Thisse, B. and Stainier, D. Y. R. (2001). *casanova* encodes a novel Sox-related protein necessary and sufficient for early endoderm formation in zebrafish. *Genes Dev.* **15**, 1493-1505.

Koopman, P., Gubbay, J., Vivian, N., Goodfellow, P. and Lovell-Badge, R. (1991). Male development of chromosomally female mice transgenic for *Sry*. *Nature* **351**, 117-121.

Lawson, K. A. and Pedersen, R. A. (1987). Cell fate, morphogenetic movement and population kinetics of embryonic endoderm at the time of germ layer formation in the mouse. *Development* **101**, 627-652.

Lu, C. C., Brennan, J. and Robertson, E. J. (2001). From fertilization to gastrulation: axis formation in the mouse embryo. *Curr. Opin. Genet. Dev.* **11**, 384-392.

Martinez Barbera, J. P., Clements, M., Thomas, P., Rodriguez, T., Meloy, D., Kioussis, D. and Beddington, R. S. (2000). The homeobox gene *Hex* is required in definitive endodermal tissues for normal forebrain, liver and thyroid formation. *Development* **127**, 2433-2445.

Maye, P., Becker, S., Kasameyer, E., Byrd, N. and Grabel, L. (2000). Indian hedgehog signaling in extraembryonic endoderm and ectoderm differentiation in ES embryoid bodies. *Mech. Dev.* **94**, 117-132.

Molkentin, J. D., Lin, Q., Duncan, S. A. and Olson, E. N. (1997). Requirement of the transcription factor GATA4 for heart tube formation and ventral morphogenesis. *Genes Dev.* **11**, 1061-1072.

Monaghan, A. P., Kaestner, K. H., Grau, E. and Schutz, G. (1993). Postimplantation expression patterns indicate a role for the mouse forkhead/HNF-3 alpha, beta and gamma genes in determination of the definitive endoderm, chordamesoderm and neuroectoderm. *Development* **119**, 567-578.

Motoyama, J., Heng, H., Crackower, M. A., Takabatake, T., Takeshima, K., Tsui, L. C. and Hui, C. (1998). Overlapping and non-overlapping Ptch2 expression with Shh during mouse embryogenesis. *Mech. Dev.* **78**, 81-84.

Narita, N., Bielinska, M. and Wilson, D. B. (1997). Wild-type endoderm abrogates the ventral developmental defects associated with GATA-4 deficiency in the mouse. *Dev. Biol.* **189**, 270-274.

Nishiguchi, S., Wood, H., Kondoh, H., Lovell-Badge, R. and Episkopou, V. (1998). Sox1 directly regulates the gamma-crystallin genes and is essential for lens development in mice. *Genes Dev.* **12**, 776-781.

Offield, M. F., Jetton, T. L., Labosky, P. A., Ray, M., Stein, R. W., Magnuson, M. A., Hogan, B. L. and Wright, C. V. (1996) PDX-1 is required for pancreatic outgrowth and differentiation of the rostral duodenum. *Development* **122**, 983-995.

Pennisi, D., Gardner, J., Chambers, D., Hosking, B., Peters, J., Muscat, G., Abbott, M. C. and Koopman, P. (2000). Mutations in *Sox18* underlie cardiovascular and hair follicle defects in ragged mice. *Nat. Genet.* **24**, 434-437.

Pevny, L. H. and Lovell-Badge, R. (1997). Sox genes find their feet. *Curr. Opin. Genet. Dev.* **7**, 338-344.

Pingault, V., Bondurand, N., Kuhlbrodt, K., Goerich, D. E., Prehu, M. O., Puliti, A., Herbarth, B., Hermans-Borgmeyer, I., Legius, E., Matthijs, G. et al. (1998). *SOX10* mutations in patients with Waardenburg-Hirschsprung disease. *Nat. Genet.* **18**, 171-173.

Ramalho-Santos, M., Melton, D. A. and McMahon, A. P. (2000). Hedgehog signals regulate multiple aspects of gastrointestinal development. *Development* **127**, 2763-2772.

Reiter, J. F., Kikuchi, Y. and Stainier, D. Y. (2001). Multiple roles for Gata5 in zebrafish endoderm formation. *Development* **128**, 125-135.

Sakaguchi, T., Kuroiwa, A. and Takeda, H. (2001). A novel sox gene, 226D7, acts downstream of Nodal signaling to specify endoderm precursors in zebrafish. *Mech. Dev.* **107**, 25-38.

Sasaki, H. and Hogan, B. L. (1993). Differential expression of multiple fork head related genes during gastrulation and axial pattern formation in the mouse embryo. *Development* **118**, 47-59.

Schilham, M. W., Oosterwegel, M. A., Moerer, P., Ya, J., de Boer, P. A., van de Wetering, M., Verbeek, S., Lamers, W. H., Kruisbeek, A. M., Cumano, A. and Clevers, H. (1996). Defects in cardiac outflow tract formation and pro-B-lymphocyte expansion in mice lacking *Sox-4*. *Nature* **380**, 711-714.

Shawlot, W., Deng, J. M. and Behringer, R. R. (1998). Expression of the mouse cerberus-related gene, Cerr1, suggests a role in anterior neural induction and somitogenesis. *Proc. Natl. Acad. Sci. USA* **95**, 6198-6203.

Simeone, A., Acampora, D., Gulisano, M., Stornaiuolo, A. and Boncinelli, E. (1992). Nested expression domains of four homeobox genes in developing rostral brain. *Nature* **358**, 687-690.

Smits, P., Li, P., Mandel, J., Zhang, Z., Deng, J. M., Behringer, R. R., de Crombrugghe, B. and Lefebvre, V. (2001). The transcription factors L-Sox5 and Sox6 are essential for cartilage formation. *Dev. Cell* **1**, 277-290.

Southard-Smith, E. M., Kos, L. and Pavan, W. J. (1998). *Sox10* mutation disrupts neural crest development in Dom Hirschsprung mouse model. *Nat. Genet.* **18**, 60-64.

Sukegawa, A., Narita, T., Kameda, T., Saitoh, K., Nohno, T., Iba, H., Yasugi, S., Fukuda, K. (2000) The concentric structure of the developing gut is regulated by Sonic hedgehog derived from endodermal epithelium. *Development* **127**, 1971-1980.

Sun, X., Meyers, E. N., Lewandoski, M. and Martin, G. R. (1999). Targeted disruption of *Fgf8* causes failure of cell migration in the gastrulating mouse embryo. *Genes Dev.* **13**, 1834-1846.

Tajima, Y., Moore, M. A. S., Soares, V., Ono, M., Kissel, H. and Besmer, P. (1998). Consequences of exclusive expression in vivo of kit-ligand lacking the major proteolytic cleavage site. *Proc. Natl. Acad. Sci. USA* **95**, 11903-11908.

Tam, P. P. and Beddington, R. S. (1992). Establishment and organization of germ layers in the gastrulating mouse embryo. *Ciba Found. Symp.* **165**, 27-49.

Taniguchi, K., Hiraoka, Y., Ogawa, M., Sakai, Y., Kido, S. and Aiso, S. (1999). Isolation and characterization of a mouse SRY-related cDNA, mSox7. *Biochim. Biophys. Acta* **1445**, 225-231.

Tremblay, K. D., Hoodless, P. A., Bikoff, E. K. and Robertson, E. J. (2000). Formation of the definitive endoderm in mouse is a Smad2-dependent process. *Development* **127**, 3079-3090.

Vidal, V. P., Chaboissier, M. C., de Rooij, D. G. and Schedl, A. (2001). *Sox9* induces testis development in XX transgenic mice. *Nat. Genet.* **28**, 216-217.

Wagner, T., Wirth, J., Meyer, J., Zabel, B., Held, M., Zimmer, J., Pasantes, J., Bricarelli, F. D., Keutel, J., Hustert, E. et al. (1994). Autosomal sex reversal and campomelic dysplasia are caused by mutations in and around the *SRY*-related gene *SOX9*. *Cell* **79**, 1111-1120.

Wegner, M. (1999). From head to toes: the multiple facets of Sox proteins. *Nucleic Acids Res.* **27**, 1409-1420.

Wells, J. M. and Melton, D. A. (1999). Vertebrate endoderm development. *Annu. Rev. Cell Dev. Biol.* **15**, 393-410.

Withington, S., Beddington, R. and Cooke, J. (2001). Foregut endoderm is required at head process stages for anteriormost neural patterning in chick. *Development* **128**, 309-320.

Wood, H. B. and Episkopou, V. (1999). Comparative expression of the mouse *Sox1*, *Sox2* and *Sox3* genes from pre-gastrulation to early somite stages. *Mech. Dev.* **86**, 197-201.

Yamaguchi, T. P., Harpal, K., Henkemeyer, M. and Rossant, J. (1994). fgfr-1 is required for embryonic growth and mesodermal patterning during mouse gastrulation. *Genes Dev.* **8**, 3032-3044.

Yamamoto, M., Meno, C., Sakai, Y., Shiratori, H., Mochida, K., Ikawa, Y., Saijoh, Y. and Hamada, H. (2001). The transcription factor FoxH1 (FAST) mediates Nodal signaling during anterior-posterior patterning and node formation in the mouse. *Genes Dev.* **15**, 1242-1256.

Zhang, X. M., Ramalho-Santos, M. and McMahon, A. P. (2001). Smoothened mutants reveal redundant roles for Shh and Ihh signaling including regulation of L/R asymmetry by the mouse node. *Cell* **105**, 781-792.